Optimized control of multistate quantum systems by composite pulse sequences

G. T. Genov, B. T. Torosov, and N. V. Vitanov

Phys. Rev. A **84**, 063413 — Published 14 December 2011

DOI: 10.1103/PhysRevA.84.063413

Optimized control of multistate quantum systems by composite pulse sequences

G. T. Genov,[1] B. T. Torosov,[1,2] and N. V. Vitanov[1]

[1]*Department of Physics, Sofia University, James Bourchier 5 blvd, 1164 Sofia, Bulgaria*
[2]*Institute of Solid State Physics, Bulgarian Academy of Sciences, Tsarigradsko chaussée 72, 1784 Sofia, Bulgaria.*

We introduce a technique for derivation of high-fidelity composite pulse sequences for two types of multistate quantum systems: systems with the SU(2) and Morris-Shore dynamic symmetries. For the former type, we use the Majorana decomposition to reduce the dynamics to an effective two-state system, which allows us to find the propagator analytically and use the pool of available composite pulses for two-state systems. For the latter type of multistate systems, we use the Morris-Shore decomposition, which reduces the multistate dynamics to a set of two-state systems. We present examples which demonstrate that the multistate composite sequences open a variety of possibilities for coherent control of quantum systems with multiple states.

PACS numbers: 32.80.Qk, 32.80.Xx 82.56.Jn, 42.50.Dv

I. INTRODUCTION

Composite pulse sequences have been used for several decades in nuclear magnetic resonance [1–8], and since recently, in quantum optics [9, 10] and quantum information processing [11–14] as a versatile control tool for two-state quantum systems. A composite pulse is a sequence of pulses with well defined relative phases between each other. These phases are used as control parameters in order to compensate particular imperfections in the excitation profile of a single pulse. These imperfections may originate from an imprecise pulse area (e.g., due to fluctuating field intensity and/or pulse duration, spatial inhomogeneity of the field, etc.), undesirable frequency offset (e.g., due to uncompensated electric and magnetic fields, Stark shifts, Doppler shifts, etc.), frequency chirping, etc. Because composite pulses preserve and expand the high-fidelity excitation range of interest, they may be viewed as combining the advantages of single resonant pulses (high fidelity) and adiabatic techniques (robustness against variations in experimental parameters). Moreover, composite pulses can improve the fidelity of adiabatic techniques well beyond the fault tolerant quantum computing benchmark [15]. Composite pulses can be used also to shape the excitation profile in essentially any desired manner, an objective which cannot be achieved with resonant pulses and adiabatic techniques.

We note that the idea of composite sequences has been developed first in polarization optics in the research on achromatic polarization retarders [16]. Such retarders are formed by several ordinary wave plates of the same or different material. West and Makas [17] described achromatic combinations of plates with different dispersions of birefringence, while achromatic retarders composed of wave plates of the same material but different thicknesses were proposed by Destriau and Prouteau [18] for two birefringent plates and Pancharatnam for three plates [19]. Later Harris and co-workers proposed achromatic retarders with 6 and 10 identical zero-order quarter-wave plates [20, 21].

Composite pulse sequences have been developed and used almost entirely for two-state quantum systems. Studies of higher dimensional systems are limited to just three states [22]. In this paper, we construct composite pulses for two classes of multistate quantum systems: systems with SU(2) dynamic symmetry [23] and systems, which are reducible by the Morris-Shore (MS) transformation [24]. We illustrate the applications of these multistate composite with explicit examples of two types of three-state quantum systems. For systems with the SU(2) dynamic symmetry we use the Majorana decomposition [23, 25] to reduce the dynamics to an effective two-state system, which allows us to find the N-state propagator analytically and use the pool of available composite pulses for two-state systems. The three-state system with the SU(2) dynamic symmetry has a chainwise linkage with equal couplings and equidistant detunings, as shown in Fig. 1(a). Multistate systems with MS symmetry [24] are such systems that can be cast into two manifolds of states with equal energies (in the rotating-wave approximation); couplings are allowed only between states

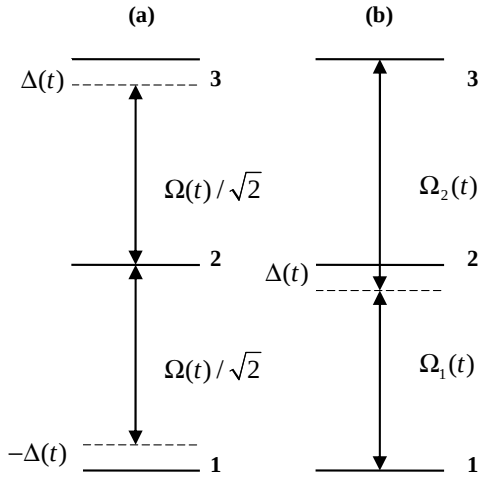

FIG. 1: (color online) Three-state chainwise connected quantum systems. (a) System with the SU(2) dynamic symmetry. (b) System with the MS symmetry (Ω_1 and Ω_2 have the same time dependance).

of different manifolds but not within the same manifold, and all couplings can be different but must have the same time dependence. The dynamics of such systems can be reduced to a set of independent two-state systems and a certain number of dark states. The most general three-state system with MS symmetry is a three-state chain on two-photon resonance (but possibly off single-photon resonance) with different couplings, as in Fig. 1(b).

This paper is organized as follows. In Sec. II, we present some general background of composite pulse sequences in two-state systems. In Sec. III, we describe the design of composite pulse sequences for multistate quantum systems with SU(2) dynamic symmetry and demonstrate compensation of pulse area and detuning deviations and selective excitation. In Sec. IV we present composite pulses for multistate systems with MS symmetry. and we illustrate their action with an example of complete population depletion in a degenerate two-level system. Sec. V discusses important issues related to the experimental feasibility of the composite pulses technique, while Sec.VI presents a summary of the results.

II. COMPOSITE PULSES IN TWO-STATE SYSTEMS

The dynamics of a two-state quantum system driven by an external coherent field is described by the Schrödinger equation,

$$i\hbar\partial_t \mathbf{c}(t) = \mathbf{H}(t)\mathbf{c}(t), \tag{1}$$

where the vector $\mathbf{c}(t) = [c_1(t), c_2(t)]^T$ contains the probability amplitudes of the two states. The Hamiltonian in the rotating-wave approximation (RWA) is

$$\mathbf{H}(t) = \frac{\hbar}{2}\begin{bmatrix} -\Delta(t) & \Omega(t) \\ \Omega^*(t) & \Delta(t) \end{bmatrix}, \tag{2}$$

where $\Delta = \omega_0 - \omega$ is the detuning between the laser carrier frequency ω and the Bohr transition frequency ω_0. The Rabi frequency $\Omega(t) = -\mathbf{d}\cdot\mathbf{E}(t)/\hbar$ parameterizes the coupling between the electric field $\mathbf{E}(t)$ and the transition dipole moment $\mathbf{d}$. Both $\Omega(t)$ and $\Delta(t)$ can be time-dependent in general. The evolution of the system is described by the propagator $\mathbf{U}$, which connects the values of the amplitudes at the initial and final times t_i and t_f: $\mathbf{c}(t_f) = \mathbf{U}(t_f, t_i)\mathbf{c}(t_i)$. The propagator is conveniently parameterized with the complex Cayley-Klein parameters a and b as

$$\mathbf{U} = \begin{bmatrix} a & b \\ -b^* & a^* \end{bmatrix}. \tag{3}$$

On exact resonance ($\Delta = 0$), the Cayley-Klein parameters depend on the pulse area $A = \int_{t_i}^{t_f} |\Omega(t)|dt$ only:

$$a = \cos(A/2), \quad b = -i\sin(A/2). \tag{4}$$

A constant phase shift ϕ in the Rabi frequency $\Omega(t)$,

$$\Omega(t) \to \Omega(t)e^{i\phi}, \tag{5}$$

is imprinted in the propagator as [9]

$$\mathbf{U}(\phi) = \begin{bmatrix} a & be^{i\phi} \\ -b^*e^{-i\phi} & a^* \end{bmatrix}. \tag{6}$$

The propagator for a composite sequence of n pulses, each having a phase ϕ_k and a pulse area A_k, reads

$$\begin{aligned}\mathbf{U}^{(n)} &= \mathbf{U}(\phi_n, A_n)\cdots\mathbf{U}(\phi_2, A_2)\mathbf{U}(\phi_1, A_1) \\ &= \begin{bmatrix} U_{11}^{(n)} & U_{12}^{(n)} \\ -[U_{12}^{(n)}]^* & [U_{11}^{(n)}]^* \end{bmatrix}.\end{aligned} \tag{7}$$

The composite phases $\phi_1, \phi_2, \ldots \phi_n$ are free control parameters, which are selected from the conditions to shape up the excitation profile in a desired manner.

A. Pulse area compensation

The most common composite pulse sequences in two-state systems are the "composite-π" pulses, which produce complete population inversion, i.e. $U_{11}^{(n)} = 0$ and $|U_{12}^{(n)}| = 1$, and "composite-$\pi/2$" pulses, which produce equal coherent superpositions, i.e. $|U_{11}^{(n)}| = |U_{12}^{(n)}| = 1/\sqrt{2}$. The composite-$\pi$ pulses are of three basic types: broadband (BB), narrowband (NB), and passband (PB) [7]. It is convenient to impose the "anagram" condition $\mathbf{H}_k(t) = \mathbf{H}_{n+1-k}(t)$, where $k = 1, 2, \ldots, n$, for it creates smooth symmetric excitation profiles [9]. Usually, the global phase of the composite pulse is irrelevant, so it is convenient to set $\phi_1 = \phi_n = 0$. The phases for these "anagram" composite pulses are derived in the following way: for BB pulses we aim to achieve a flat top of the excitation profile at pulse area $A = \pi$; for NB pulses we require a flat bottom at $A = 0$ (or $A = 2\pi$); for PB pulses we need both a flat top at $A = \pi$ and a flat bottom at $A = 0$. These requirements lead to the following conditions [9]:

$$\text{BB: } \left[\partial_A^k U_{11}^{(n)}\right]_{A=\pi} = 0 \ (k = 1, 3, \ldots, n-2); \tag{8a}$$

$$\text{NB: } \left[\partial_A^k U_{11}^{(n)}\right]_{A=0} = 0 \ (k = 2, 4, \ldots, n-1); \tag{8b}$$

$$\text{PB: } \left[\partial_A^k U_{11}^{(n)}\right]_{A=\pi} = 0 \ (k = 1, 3, \ldots, l), \tag{8c}$$

$$\left[\partial_A^k U_{11}^{(n)}\right]_{A=0} = 0 \ (k = 2, 4, \ldots, n-l-2); \tag{8d}$$

where $\partial_A^k \equiv \partial^k/\partial A^k$. The omitted derivatives vanish identically [9]. The number of vanishing derivatives at the particular value of the pulse area determines the "flatness" of the excitation profile there.

The phases for the BB composite sequences are given by the following simple formula [9]:

$$\phi_k^{(n)} = \left(n + 1 - 2\left\lfloor\frac{k+1}{2}\right\rfloor\right)\left\lfloor\frac{k}{2}\right\rfloor\frac{\pi}{n}, \tag{9}$$

with $k = 1, 2, \ldots, n$. No such formula exists for the NB and PB sequences, except for a small number of ingredient pulses, and their phases are found numerically [9].

B. Detuning compensation

Composite pulses can also be used to stabilize the excitation against variations in the detuning. The approach is similar to pulse area compensation but now the composite phases are determined from the condition that the first few derivatives of the propagator elements vs the detuning vanish. The Cayley-Klein parameters a and b for each ingredient pulse now depend not only on the pulse area but on the detuning and the pulse shape too, and in general, the composite phases are different for different pulse shapes [9]. For composite sequences of up to five pulses and time-symmetric pulse shapes, however, the composite phases are universal [9].

The m independent phases of an "anagram" BB composite sequence of $n = 2m + 1$ pulses for detuning compensation are derived from the following set of algebraic equations:

$$\left[\partial_\Delta^k U_{11}^{(n)}\right]_{\Delta=0} = 0 \quad (k = 0, 1, ..., m-1); \tag{10}$$

There are multiple solutions in general, with different excitation profiles.

Composite pulse sequences can compensate simultaneous pulse area and detuning variations; the composite phases are determined by nullifying the first few mixed partial derivatives of the propagator elements:

$$\left[\frac{\partial^{k+l} U_{11}^{(n)}}{\partial A^k \partial \Delta^l}\right]_{A=\pi,\Delta=0} = 0, \tag{11}$$

where k and l determine the flatness vs the pulse area A and the detuning Δ, respectively. Again, we determine the phases of the constituent pulses from the resulting set of algebraic equations.

These and other composite pulse sequences applicable to two-state quantum systems can be applied to multistate systems that can be reduced to effective two-state systems, as we show in the following sections.

III. SYSTEMS WITH SU(2) DYNAMIC SYMMETRY

A. General Theory

The elements of the Hamiltonian for a multistate system with SU(2) dynamic symmetry read [26, 27]

$$H_{kk}(t) = \hbar m \Delta(t), \tag{12a}$$

$$H_{k,k+1}(t) = H_{k+1,k}(t)^* = \frac{\hbar}{2}\Omega(t)\sqrt{k(N-k)}, \tag{12b}$$

$$H_{kl}(t) = 0, \qquad (|k-l| \geq 2), \tag{12c}$$

where $k = 1, 2, ..., N$ and $m = k-(N+1)/2$. The linkage pattern is a chain, in which all couplings (the off-diagonal elements) are proportional to $\Omega(t)$ and thus share the same time dependence, but have different magnitudes. The detunings (the diagonal elements) are equidistant and proportional to Δ. The propagator of the multistate system can be expressed by the propagator of an effective two-state system, with the Hamiltonian of Eq. (2) [23, 26, 27], i.e. in terms of the two-state Cayley-Klein parameters a and b of Eq. (6),

$$U_{jk} = \sum_l \frac{[(N-j)!(j-1)!(N-k)!(k-1)!]^{1/2}}{l!q!r!s!} a^l (a^*)^q b^r (-b^*)^s, \tag{13}$$

where $q = j+k+l-N-1$, $r = N-j-l$, $s = N-k-l$, and l is a non-negative integer that runs over all values for which all factorial functions are defined. If the initial condition for the multistate system is $\mathbf{b}(t_i) = [1, 0, ..., 0]^T$, then the initial condition for the corresponding two-state system is $\mathbf{c}(t_i) = [1, 0]^T$ [27]. Of particular interest is the probability for transition between the two ends of the chain, $P_{1\to N} = |U_{N1}|^2$, which is readily calculated from Eq. (13):

$$P_{1\to N} = |b|^{2(N-1)} = p^{N-1}, \tag{14}$$

where $p = |b|^2$ is the transition probability for the two-state system described by the Hamiltonian of Eq. (2). Therefore, complete population transfer $1 \to 2$ in the two-state problem implies complete population transfer $1 \to N$ in the N-state problem. However, the sensitivity to variations in the interaction parameters is greatly amplified, at the power of $(N-1)$, in the N-state system.

The evolution of the N-state system induced by a composite pulse sequence can be derived from Eqs.(7) and (13) with the replacement $a \to U_{11}^{(n)}$ and $b \to U_{12}^{(n)}$ in the latter.

B. SU(2)-symmetric three-state system

The three-state system in Fig. 1(a) is the simplest nontrivial example of a multistate system with the SU(2) dynamic symmetry. The Hamiltonian of this system is given by Eq. (12) and reads explicitly

$$\mathbf{H} = \hbar \begin{bmatrix} -\Delta(t) & \frac{1}{\sqrt{2}}\Omega(t) & 0 \\ \frac{1}{\sqrt{2}}\Omega^*(t) & 0 & \frac{1}{\sqrt{2}}\Omega(t) \\ 0 & \frac{1}{\sqrt{2}}\Omega^*(t) & \Delta(t) \end{bmatrix}. \tag{15}$$

Given the propagator in Eq. (3), which describes the evolution of the corresponding two-state system, the respective propagator for the three-state system is

$$\mathbf{U}_3 = \begin{bmatrix} a^2 & \sqrt{2}ab & b^2 \\ -\sqrt{2}ab^* & |a|^2 - |b|^2 & \sqrt{2}a^*b \\ -b^{*2} & -\sqrt{2}a^*b^* & a^{*2} \end{bmatrix}. \tag{16}$$

The evolution of this three-state system subjected to a composite pulse sequence is described by Eq. (16) with the replacement $a \to U_{11}^{(n)}$ and $b \to U_{12}^{(n)}$.

C. Applications

1. Pulse Area Compensation

According to Eq. (14), a single resonant generalized π-pulse gives probability $P_{1\to N} = 1$. Here the pulse area is defined as the time integral over the Rabi frequency "unit" $\Omega(t)$ in Eq. (12), $A = \int_{t_i}^{t_f} |\Omega(t)|dt$. For small deviation ϵ from this area, $A = \pi(1+\epsilon)$, the transition probability behaves as

$$P_{1\to N} \sim 1 - (N-1)\frac{\pi^2\epsilon^2}{4} + \mathcal{O}(\epsilon^4). \qquad (17)$$

BB composite pulse sequences can greatly reduce this sensitivity to an arbitrarily high order of ϵ. For the anagram BB sequences with the analytic phases of Eq. (9), the two-state transition probability p for a sequence of n pulses is exactly given by [9, 15]

$$p = 1 - a^{2n} = 1 - \cos^{2n}(A/2); \qquad (18)$$

hence the inversion probability in the SU(2)-symmetric N-state system is

$$P_{1\to N} = [1 - \cos^{2n}(A/2)]^{N-1}. \qquad (19)$$

For small deviations from the desired area of a generalized π-pulse, $A = \pi(1+\epsilon)$, we find

$$P_{1\to N} \sim 1 - (N-1)\left(\frac{\pi\epsilon}{2}\right)^{2n} + \mathcal{O}(\epsilon^{2n+2}). \qquad (20)$$

Equation (20) shows that an arbitrarily large deviation ϵ can always be compensated with sufficiently long composite sequences.

Figure 2 illustrates the stabilization of the transition probability $P_{1\to N}$ against variations in the pulse area A for three- and five-state SU(2)-symmetric systems. Even the three-pulse composite sequence greatly broadens the range of areas wherein $P_{1\to N} \approx 1$. Longer composite sequences allow us to compensate larger variations of the pulse area: the transition probability is kept above 99% for up to 35% variations in A with $n = 5$ pulses, and up to 60% variations in A with $n = 15$ pulses. For larger systems (with a larger number of states N), the excitation profile shrinks, as predicted by Eq. (20).

NB and PB composite pulse sequences can be used also to increase selectivity of excitation in SU(2)-symmetric multistate quantum systems in a similar manner as in two-state systems [10]. Such sequences can produce arbitrarily narrow excitation profile (NB pulses) or a combination of BB and NB features (PB pulses). NB composite sequences, in particular, suppress excitation in the wings

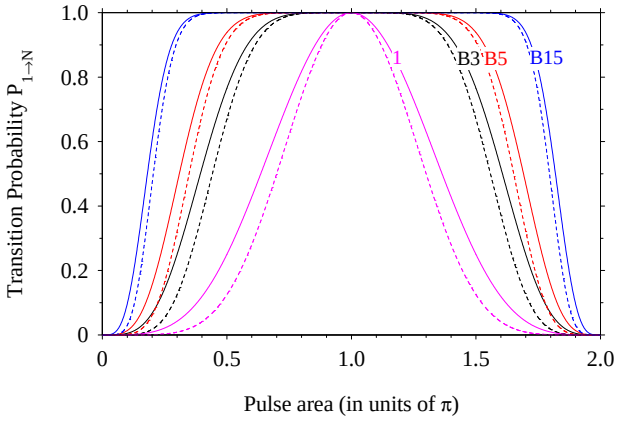

FIG. 2: (color online) Transition probability $P_{1\to N}$ for three- and five-state systems with SU(2) dynamic symmetry, described by the Hamiltonian of Eq. (12), vs the pulse area A for a single pulse and for composite sequences of 3, 5 and 15 pulses (denoted on the curves), with phases from Eq. (9). Solid curves: $N = 3$ states; dashed curves: $N = 5$ states.

of the excitation profile, thereby shrinking the excitation to a narrower range of pulse areas than the excitation range of single pulse; this feature allows improved local addressing of closely spaced trapped atoms [10].

An example for the application of BB and PB pulses in SU(2)-symmetric multistate systems is demonstrated in Fig. 3. An arbitrarily narrow excitation profiles can be obtained with sufficiently long NB composite sequences. The PB composite sequences both suppress excitation for pulse areas around the values 0 and 2π and enhance excitation for pulse areas around π; thereby creating a sort of "rectangular" excitation profiles.

2. Detuning Compensation

Because of the correspondence of SU(2)-symmetric multistate systems to the two-state system, Eq. (13), which is particularly simple for the probability $P_{1\to N}$, Eq. (14), composite pulse sequences can be used to stabilize the excitation profile against variations in the detuning Δ, in a similar manner as in two-state systems [9]. As it is well known, the transition probability decreases in a polynomial manner with Δ for rectangular pulses, and in an exponential manner for smooth pulse shapes [28–30].

We consider composite sequences of pulses with hyperbolic-secant shape and constant detuning (known as the Rosen-Zener model [28]):

$$\Omega(t) = \Omega_0 \mathrm{sech}(t/T), \qquad \Delta(t) = \mathrm{const}. \qquad (21)$$

The two-state transition probability for a single sech pulse is well known[28],

$$p = \sin^2(\pi\Omega_0 T/2)\mathrm{sech}^2(\pi\Delta T/2), \qquad (22)$$

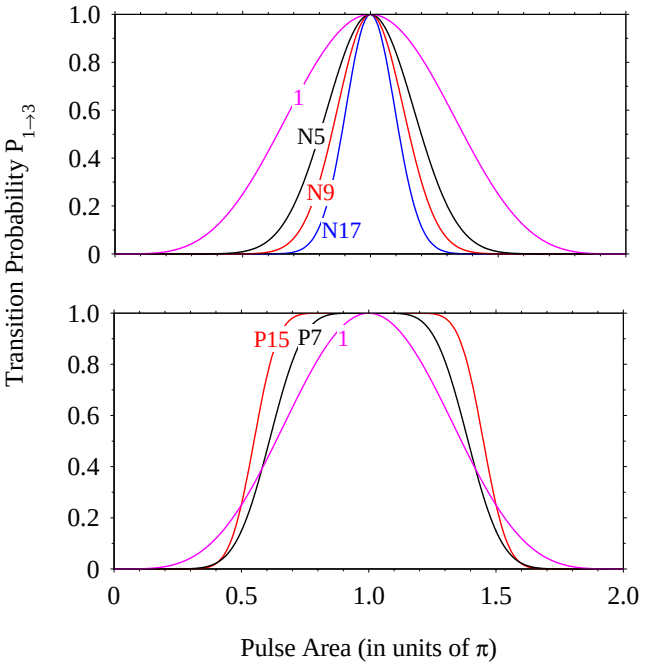

FIG. 3: (color online) Transition probability $P_{1\to 3}$ for a three-state system with SU(2) dynamic symmetry, described by the Hamiltonian of Eq. (15), vs the pulse area A for a single pulse and for NB composite sequences of 5, 9 and 17 pulses (denoted on the curves) (top frame), and PB composite sequences of 7 and 15 pulses (bottom frame) with phases (approx.) [9]:
N5: $(0, 1.161, 0.580, 1.161, 0)\pi$;
N9: $(0, 1.129, 0.822, 0.108, 1.386, 0.108, 0.822, 1.129, 0)\pi$;
N17: $(0, 1.604, 0.553, 1.091, 0.888, 0.620, 1.535, 0.149, 1.569, 0.149, 1.535, 0.620, 0.888, 1.091, 0.553, 1.604, 0)\pi$;
P7: $(0, 0.704, 1.186, 1.834, 1.186, 0.704, 0)\pi$;
P15: $(0, 0.473, 0.421, 1.624, 1.050, 1.081, 1.469, 0.259, 1.469, 1.081, 1.050, 1.624, 0.421, 0.473, 0)\pi$.

and the transition probability between the two ends of a SU(2)-symmetric chain can be found from Eq. (14): $P_{1\to N} = p^{N-1}$. Complete population transfer $|1\rangle \to |N\rangle$ is achieved for $\Omega_0 T = 1$ and $\Delta = 0$. However, as the detuning Δ departs from zero, the transition probability for a sech pulse of area π (i.e., $\Omega_0 T = 1$) decreases as

$$P_{1\to N} \sim 1 - (N-1)\frac{\pi^2 T^2}{4}\Delta^2 + \mathcal{O}(\Delta^4). \qquad (23)$$

(For large Δ the transition probability vanishes exponentially, as Eq. (22) shows.)

Various composite sequences can be derived from conditions (10) . Using the results in Ref. [9], we find that the composite sequence of three pulses with areas π (i.e., $\Omega_0 T = 1$) and phases $(0, \pi/3, 0)$ compensates the second-order deviation,

$$P_{1\to N} \sim 1 - (N-1)\frac{(\pi T^2 \ln 2)^2}{4}\Delta^4 + \mathcal{O}(\Delta^6), \qquad (24)$$

while the sequence of five π-pulses with phases $\phi_1 = 0, \phi_2 = \pi/6, \phi_3 = -\pi/3, \phi_4 = \pi/6, \phi_5 = 0$ compensates

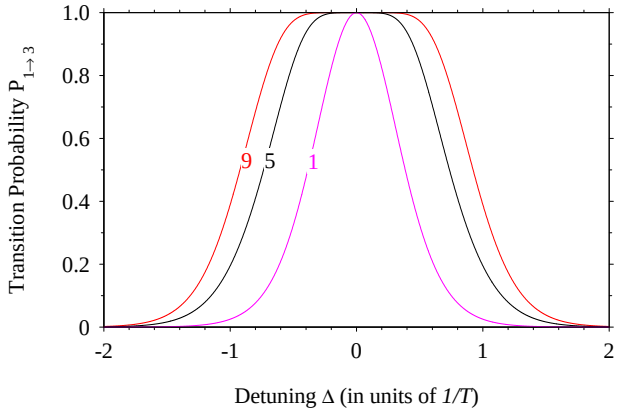

FIG. 4: (color online) Transition probability $P_{1\to 3}$ for a three-state system with SU(2) symmetry versus the detuning for a single hyperbolic-secant pulse and for a sequence of five $3\pi/5$ pulses with phases (approximately) $(0, 0.747, 0.424, 0.747, 0)\pi$ and nine $4\pi/9$ pulses with phases (approximately) $(0, 1.308, 1.153, 1.251, 0.562, 1.251, 1.153, 1.308, 0)\pi$.

the detuning up to sixth order,

$$P_{1\to N} \sim 1 - \mathcal{O}(\Delta^6). \qquad (25)$$

The stabilization of the transition probability vs the detuning is demonstrated in Fig. 4. Compensation to an arbitrary order can be achieved with a sufficiently long composite sequence. Note that the individual pulse areas need not equal π; indeed, the pulse areas for the five- and nine-pulse sequences in Fig. 4 are considerably less than π.

Composite pulse sequences can be used to stabilize the transition probability against variations in both pulse area and detuning; various sets of composite phases can be derived from conditions (11). An example of such simultaneous compensation of area and detuning variations is shown in Fig. 5. The high-excitation area in the (Δ, Ω_0) plane is greatly expanded by just a five-pulse composite sequence.

IV. SYSTEMS WITH MORRIS-SHORE SYMMETRY

A. General Theory

In this section we shall demonstrate the potential applications of composite pulses in multistate quantum systems with MS symmetry, i.e., systems amenable to the MS decomposition [24, 31]. These systems obey three conditions: (i) their states can be cast into two sets with the same RWA energies, 0 or $\hbar\Delta$, the implication being that any two states of the same set are on two-photon resonance; (ii) couplings exist between states of different sets but not within the same set, i.e., $\Omega_{jk} = 0$ if states $|j\rangle$ and $|k\rangle$ are in the same set, and (iii) all couplings

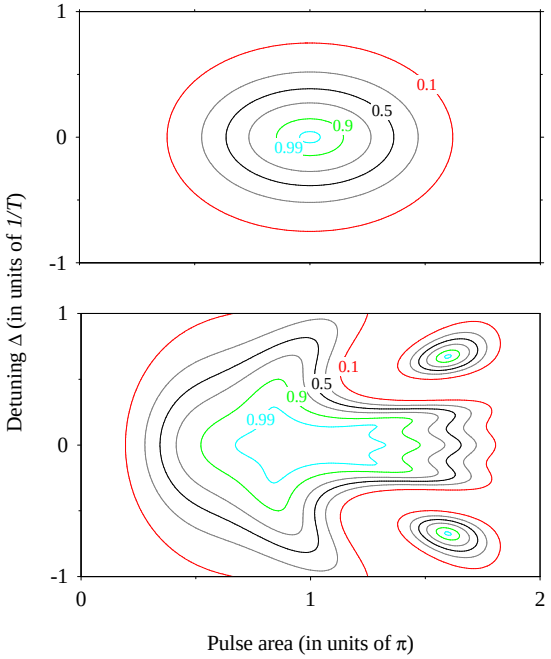

FIG. 5: (color online) Contour plots of the transition probability $P_{1\to 3}$ with respect to pulse area and the detuning for a single pulse (top) and composite pulse of five pulses with phases $(0, 5/6, 1/3, 5/6, 0)\pi$.

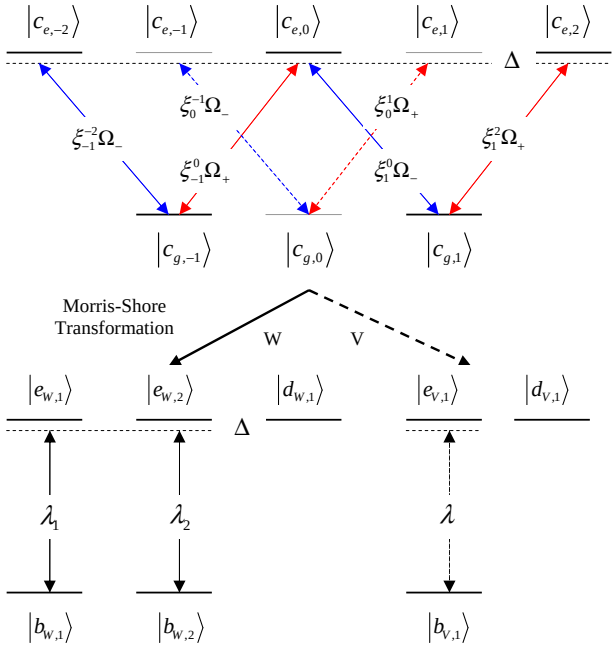

FIG. 6: (color online) Morris-Shore transformation of a W-system ($N_a = 3$, $N_b = 2$) and a V-system ($N_a = 2$, $N_b = 1$), which are independent from each other. The W-system is transformed into two independent two-state systems with couplings λ_1 and λ_2 and a dark state. The V-system itself is transformed into one independent two-state system with coupling λ and a second dark state.

can be different but they must have the same time dependence $f(t)$. The dynamics of such systems can be reduced to a set of independent two-state systems and a certain number of dark states. We assume without loss of generality that the two sets contain N_a and N_b states, where $N = N_a + N_b$ and $N_a \geqq N_b$. Then the application of the MS transformation reduces the system to N_b independent two-state systems and $N_a - N_b$ dark states [24, 31].

The three-state system with MS symmetry has a chain linkage and is on two-photon resonance, but may have a single-photon detuning and different couplings, as shown in Fig. 1(b). An eight-state example of an MS-symmetric system is illustrated in Fig. 6 for $N_a = 3$ and $N_b = 5$.

The dynamics of an MS-symmetric N-state quantum system is given by the solution of the Schrodinger equation (1), with $\mathbf{c}(t) = [c_1(t), c_2(t), ..., c_N(t)]^T$. We order the states in such a way that the set with the RWA energy 0 comes first followed by the other set, with the RWA energy $\hbar\Delta$. Then the Hamiltonian can be written in a block-matrix form,

$$\mathbf{H}(t) = \hbar \begin{bmatrix} \mathbf{0} & \mathbf{V}f(t) \\ \mathbf{V}^\dagger f(t) & \mathbf{D}(t) \end{bmatrix}. \tag{26}$$

Here $\mathbf{0}$ is an N_a-dimensional square zero matrix; the zero off-diagonal elements indicate the absence of couplings between the states in this manifold, while the zero diagonal elements show that these states have the same RWA energy, which is taken to be 0 without loss of generality.

The matrix $\mathbf{D}(t)$ is an N_b-dimensional diagonal matrix with equal diagonal elements, i. e. $\mathbf{D}(t) = \Delta(t)\mathbf{1}$; again, the zero off-diagonal elements reflect the absence of couplings within this set of states. Finally, the matrix $\mathbf{V}$ is an $(N_a \times N_b)$-dimensional interaction matrix,

$$\mathbf{V} = \begin{bmatrix} \Omega_{11} & \Omega_{12} & \cdots & \Omega_{1N_b} \\ \Omega_{21} & \Omega_{22} & \cdots & \Omega_{2N_b} \\ \vdots & \vdots & \vdots & \vdots \\ \Omega_{N_a1} & \Omega_{N_a2} & \cdots & \Omega_{N_aN_b} \end{bmatrix}. \tag{27}$$

We note that $V_{jk} = \Omega_{jk}$, where $\Omega_{jk} f(t) = -\mathbf{d_{jk}} \cdot \mathbf{E}(t)/2\hbar$ represents the coupling between the j-th state in the set of N_a states and the k-th state in the set of N_b states after rearrangement, so we can write the Hamiltonian in the form of Eq. (26). If the same phase shift is applied to all couplings, i.e., $\Omega_{jk} \to \Omega_{jk} e^{i\phi}$, the interaction matrix is phase shifted too, $\mathbf{V}(\phi) = \mathbf{V}e^{i\phi}$.

This multistate system can be reduced with a constant unitary transformation $\mathbf{S}$ — the MS transformation — to an equivalent system, which consists of N_b independent two-state systems and $N_d = N_a - N_b$ uncoupled (dark) states ($N_a \geqq N_b$). The transformation of the probability amplitudes reads [24, 32] $\widetilde{\mathbf{c}} = \mathbf{S}\mathbf{c}$, where tildes denote variables in the MS basis $\{|\widetilde{\psi}_k\rangle\}_{k=1}^N$ hereafter. The transformation matrix $\mathbf{S}$ is constant and has a block-diagonal

form,

$$\mathbf{S} = \begin{bmatrix} \mathbf{A} & \mathbf{0} \\ \mathbf{0} & \mathbf{B} \end{bmatrix}. \tag{28}$$

The matrix $\mathbf{A}$ is a unitary N_a-dimensional square matrix and $\mathbf{B}$ is a unitary N_b-dimensional square matrix: $\mathbf{A}\mathbf{A}^\dagger = \mathbf{A}^\dagger\mathbf{A} = \mathbf{1}_{N_a}$, and $\mathbf{B}\mathbf{B}^\dagger = \mathbf{B}^\dagger\mathbf{B} = \mathbf{1}_{N_b}$. The matrices $\mathbf{A}$ and $\mathbf{B}$ mix only states of the same set: $\mathbf{A}$ mixes the a states and $\mathbf{B}$ mixes the b states. The matrices $\mathbf{A}$ and $\mathbf{B}$ are determined from the condition that they diagonalize $\mathbf{V}\mathbf{V}^\dagger$ and $\mathbf{V}^\dagger\mathbf{V}$, respectively, and have the form [32–34]

$$\mathbf{A} = [|\widetilde{\psi}^d_1\rangle, \ldots, |\widetilde{\psi}^d_{N_d}\rangle, |\widetilde{\psi}^a_1\rangle, \ldots, |\widetilde{\psi}^a_{N_b}\rangle]^\dagger, \tag{29a}$$

$$\mathbf{B} = [|\widetilde{\psi}^b_1\rangle, \ldots, |\widetilde{\psi}^b_{N_b}\rangle]^\dagger. \tag{29b}$$

Here the set of dark states $|\widetilde{\psi}^d_1\rangle, \ldots, |\widetilde{\psi}^d_{N_d}\rangle$ and states $|\widetilde{\psi}^a_1\rangle, \ldots, |\widetilde{\psi}^a_{N_b}\rangle$ are eigenstates of $\mathbf{V}\mathbf{V}^\dagger$, while the set of states $|\widetilde{\psi}^b_1\rangle, \ldots, |\widetilde{\psi}^b_{N_b}\rangle$ are eigenstates of $\mathbf{V}^\dagger\mathbf{V}$.

Because

$$\mathbf{V}^\dagger(\phi)\mathbf{V}(\phi) = \mathbf{V}^\dagger\mathbf{V}, \tag{30a}$$

$$\mathbf{V}(\phi)\mathbf{V}^\dagger(\phi) = \mathbf{V}\mathbf{V}^\dagger, \tag{30b}$$

we conclude that the transformation $\mathbf{S}$ does not depend on the phase shift ϕ. The transformed Hamiltonian in the MS basis reads

$$\widetilde{\mathbf{H}}(\phi, t) = \mathbf{S}\mathbf{H}(\phi, t)\mathbf{S}^\dagger = \hbar \begin{bmatrix} \mathbf{0} & \widetilde{\mathbf{V}}(\phi)f(t) \\ \widetilde{\mathbf{V}}^\dagger(\phi)f(t) & \mathbf{D}(t) \end{bmatrix}, \tag{31}$$

where $\widetilde{\mathbf{V}}(\phi) = \mathbf{A}\mathbf{V}(\phi)\mathbf{B}^\dagger = \widetilde{\mathbf{V}}e^{i\phi}$. The $N_a \times N_b$-dimensional matrix $\widetilde{\mathbf{V}}$ has $N_d = N_a - N_b$ null rows. After removing these rows $\mathbf{V}$ reduces to an N_b-dimensional diagonal square matrix, whose diagonal elements can be denoted as λ_k $(k = 1, 2, ..., N_b)$; it is readily seen that λ_k^2 are the eigenvalues of $\mathbf{V}^\dagger\mathbf{V}$.

This implies that in the MS basis the system reduces to N_d decoupled (dark) states and N_b independent two-state systems, each driven by the Hamiltonian

$$\widetilde{\mathbf{H}}_k(\phi, t) = \hbar \begin{bmatrix} 0 & \lambda_k f(t)e^{i\phi} \\ \lambda_k f(t)e^{-i\phi} & \Delta(t) \end{bmatrix}. \tag{32}$$

The propagator for each of these two-state systems is

$$\widetilde{\mathbf{U}}_k(\phi) = \begin{bmatrix} a_k & b_k e^{i\phi} \\ -b_k^* e^{-i(\phi+\delta)} & a_k^* e^{-i\delta} \end{bmatrix}. \tag{33}$$

where a_k and b_k are the Cayley-Klein parameters of each of the two-state systems for $\phi = 0$ and $\delta = \int_{t_i}^{t_f} \Delta(t)dt$. The phase factor $\exp(-i\delta)$ is not important and originates from the representation of the Hamiltonian (26). The propagator for the N-state system in the MS basis is given by

$$\widetilde{\mathbf{U}}(\phi) = \begin{bmatrix} \mathbf{1}_{N_d} & \mathbf{0} & \mathbf{0} \\ \mathbf{0} & \mathbf{a} & \mathbf{b}e^{i\phi} \\ \mathbf{0} & -\mathbf{b}^* e^{-i(\phi+\delta)} & \mathbf{a}^* e^{-i\delta} \end{bmatrix}. \tag{34}$$

where $\mathbf{1}_{N_d}$ is an N_d-dimensional unit matrix, $\mathbf{a}$ is an N_b-dimensional diagonal matrix with a_k $(k = 1, \ldots, N_b)$ on the diagonal, while $\mathbf{b}$ is an N_b-dimensional diagonal matrix with b_k $(k = 1, \ldots, N_b)$ on the diagonal. Then the phased propagator in the original basis reads $\mathbf{U}(\phi) = \mathbf{S}^\dagger\widetilde{\mathbf{U}}(\phi)\mathbf{S}$, or explicitly [32, 34],

$$\mathbf{U}(\phi) = \begin{bmatrix} \mathbf{1} + \sum\limits_{k=1}^{N_b} (a_k - 1)|\widetilde{\psi}^a_k\rangle\langle\widetilde{\psi}^a_k| & \sum\limits_{k=1}^{N_b} b_k e^{i\phi}|\widetilde{\psi}^a_k\rangle\langle\widetilde{\psi}^b_k| \\ \sum\limits_{k=1}^{N_b} -b_k^* e^{-i(\phi+\delta)}|\widetilde{\psi}^b_k\rangle\langle\widetilde{\psi}^a_k| & \sum\limits_{k=1}^{N_b} a_k^* e^{-i\delta}|\widetilde{\psi}^b_k\rangle\langle\widetilde{\psi}^b_k| \end{bmatrix}. \tag{35}$$

A composite pulse sequence with phases $\phi_1, \phi_2, \ldots, \phi_n$ produces the propagator

$$\mathbf{U}^{(n)} = \mathbf{U}(\phi_n)\cdots\mathbf{U}(\phi_2)\mathbf{U}(\phi_1) = \mathbf{S}^\dagger\widetilde{\mathbf{U}}^{(n)}\mathbf{S}, \tag{36}$$

where $\widetilde{\mathbf{U}}^{(n)} = \widetilde{\mathbf{U}}(\phi_n)\cdots\widetilde{\mathbf{U}}(\phi_2)\widetilde{\mathbf{U}}(\phi_1)$ and we have used that the transformation matrix $\mathbf{S}$ does not depend on the phases ϕ_k. Hence we can find the propagator in the MS basis and apply a single transformation to the original basis. This symmetry simplifies the calculations tremendously because in the MS basis we have just N_b independent two-state systems and N_d decoupled states, and we can use the numerous BB, NB and PB composite pulses for two-state systems.

B. Example: Population inversion of degenerate levels

An interesting example of a system with Morris-Shore symmetry is the transition between the degenerate magnetic sublevels of two levels with angular momenta J_g and J_e [35] driven by elliptically polarized laser field. Because this field can be viewed as a coherent superposition of right circular (σ^+) and left circular (σ^-) polarized fields, there are two parallel linkage patterns formed of alternating lower and upper magnetic sublevels. For example, the sublevels of the two degenerate levels with angular momenta $J_g = 1$ and $J_e = 2$ in Fig. 6 form two parallel chains, resembling the letters "V" and "W". The W-shaped five-state chain is formed of the sublevels $m_g = -1$ and $m_g = 1$ of a lower ground level with angular momentum $J_g = 1$ and the sublevels $m_e = -2, 0, 2$ of an upper excited level with angular momentum $J_e = 2$. The V-shaped three-state chain is formed of the magnetic sublevels $m_g = 0$ of the lower level and the sublevels $m_e = -1$ and $m_e = 1$ of the upper level. Such a degenerate system can easily be found in various atoms. For example, the transition between the $F = 1$ hyperfine level of the $5^2S_{1/2}$ level of ^{87}Rb and the $F = 2$ hyperfine level of the $5^2P_{1/2}$ level, in the D1 line of ^{87}Rb; a similar transition is found in the D2 line of ^{87}Rb too [36]. For both parallel chains all conditions for the MS decomposition are fulfilled: two sets with the same RWA energies (the upper sublevels may be detuned by $\hbar\Delta$), no couplings within the same manifold, and the same

time dependence of all couplings since they are induced by a single (pulse-shaped) laser field. We assume that the interaction time is shorter than the decay time of the excited level (27.7ns for the D1 line of ^{87}Rb), so that no spontaneous emission and ensuing population redistribution or population loss take place. Hence, the V and W chains cannot exchange population and they evolve independently.

After the MS transformation, the W-system is decomposed into two independent two-state systems and a decoupled state, while the V system is decomposed into a two-state system and a decoupled state. The lower states of the MS two-state systems are coherent superpositions of the $J_g = 1$ sublevels, while the upper states are coherent superpositions of the $J_e = 2$ sublevels of the original system. The decoupled states are coherent superpositions of the excited sublevels of the original system. Specifically, the MS excited states and the dark state in the W system are the eigenvectors of $\mathbf{V}_W\mathbf{V}_W^\dagger$, which correspond to the nonzero eigenvalues $\lambda_{1,2}^2$ and a zero eigenvalue, respectively, while the MS ground states are the eigenvectors of $\mathbf{V}_W^\dagger\mathbf{V}_W$. Here

$$\mathbf{V}_W = \begin{bmatrix} \Omega_- e^{-i\beta_-} & 0 \\ \sqrt{\frac{1}{6}}\,\Omega_+ e^{i\beta_+} & \sqrt{\frac{1}{6}}\,\Omega_- e^{-i\beta_-} \\ 0 & \Omega_+ e^{i\beta_+} \end{bmatrix}, \tag{37}$$

where we have included the relevant Clebsch-Gordan coefficients. For the V-system, the interaction matrix is

$$\mathbf{V}_V = \begin{bmatrix} \sqrt{\frac{1}{2}}\,\Omega_- e^{-i\beta_-} \\ \sqrt{\frac{1}{2}}\,\Omega_+ e^{i\beta_+} \end{bmatrix}. \tag{38}$$

Here $\Omega_+ f(t)$ and $\Omega_- f(t)$ are real time-dependant Rabi frequencies for the couplings induced by the σ^+ and σ^- polarized laser fields, and β_+ and β_- are their phases. The couplings can be produced by a single elliptically polarized laser pulse, which is represented as a superposition of two circularly polarized σ^+ and σ^- fields: $E(t) = [E_+ e^{-i\omega t + i\beta_+} + E_- e^{i\omega t + i\beta_-}] f(t)$. The rotation angle of the polarization ellipse is $\beta = \beta_+ + \beta_-$; we choose for simplicity $\beta_- = -\beta_+ = 0$. The ellipticity is

$$\varepsilon \equiv \frac{\Omega_+^2 - \Omega_-^2}{\Omega_+^2 + \Omega_-^2} = \frac{E_+^2 - E_-^2}{E_+^2 + E_-^2}. \tag{39}$$

Then $\Omega_\pm = \Omega\sqrt{\frac{1}{2}(1 \pm \varepsilon)}$, with $\Omega = \sqrt{\Omega_+^2 + \Omega_-^2}$. The composite phases ϕ_k, which result in $\mathbf{V}(\phi_k) = \mathbf{V}e^{i\phi_k}$, can be imprinted on each elliptically polarized laser pulse by a phase shifting device, such as an accousto-optic or electro-optic modulator for microsecond and nanosecond pulses, or a pulse shaper for femtosecond pulses.

The MS eigenvalues for the W system are

$$\lambda_1 = \Omega\sqrt{\frac{7 + \sqrt{1 + 24\varepsilon^2}}{12}}, \tag{40a}$$

$$\lambda_2 = \Omega\sqrt{\frac{7 - \sqrt{1 + 24\varepsilon^2}}{12}}, \tag{40b}$$

while the MS eigenvalue for the V system is merely

$$\lambda = \Omega/\sqrt{2}. \tag{41}$$

Because for any ellipticity ε, these three couplings are incommensurate it is impossible to invert their MS systems simultaneously with a resonant pulse ($\Delta = 0$). In other words, starting with the population in an *arbitrary*, pure or mixed, superposition of the three ground sublevels, it is impossible to transfer all population to the excited sublevels with a single resonant pulse (of course, if the system is initially in a *single* magnetic ground sublevel it can easily be inverted.) However, a BB composite pulse sequence can broaden the excitation profile so much as all three couplings of Eqs. (40) and (41) will fall in the high-excitation range of the BB pulse and all population can be lifted up to the excited sublevels, *regardless of the initial state*.

For example, for linear polarization ($\varepsilon = 0$), the two MS couplings in the W system are $\lambda_1 = \Omega\sqrt{\frac{2}{3}}$, $\lambda_2 = \Omega\sqrt{\frac{1}{2}}$; altogether with the MS coupling in the V system (41) they can be put into the high-excitation range of any BB composite sequences. Figure 7 demonstrates population inversion in this degenerate system when the lower level is prepared in an equal coherent superposition of its three sublevels, for a few BB composite sequences. BB sequences clearly allow one not only to achieve high-fidelity population inversion in such systems but to have this inversion in large ranges of pulse areas. We point out that this feature remains valid for arbitrary initial conditions (including mixed states) and arbitrary light ellipticity ε. We emphasize again that with a single resonant pulse such complete inversion is impossible for arbitrary initial conditions.

V. EXPERIMENTAL FEASIBILITY

We turn now our attention to various experimental issues regarding the implementation of composite pulse sequences in real physical systems.

The first experimental restriction on the use of the composite sequences is that their duration should not exceed the decay time of the excited atomic states. This implies that the application of very long composite sequences with fixed pulse area of each constituent pulse (e.g. π) would require either long interaction times, which might exceed the spontaneous decay time of the system, or a large Rabi frequency, which might ultimately

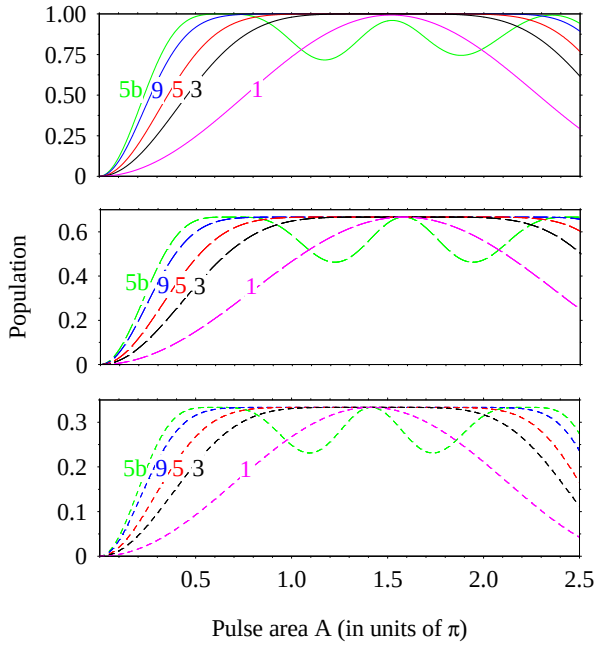

FIG. 7: (color online) Total population in the excited sublevels of a degenerate two-level system formed of the sublevels of the transition $J_g = 1 \leftrightarrow J_e = 2$ following the action of a BB resonant composite pulse sequence vs pulse area $A = 2|\Omega| \int_{t_i}^{t_f} f(t)dt$, where $\Omega = \sqrt{\Omega_+^2 + \Omega_-^2}$ (Eq. (36)). Comparison is made between the inversion induced by a single pulse and BB sequences of $n = 3, 5$, and 9 pulses with phases from Eq. (9). Additionally, a composite pulse, labeled 5b, with phases: $(0, 0.843, 2.421, 0.843, 0)$ is shown to demonstrate a composite sequence of five $3\pi/7$ pulses. The system is prepared initially in a equal coherent superposition of the ground sublevels, $|\psi_i\rangle = (|-1\rangle + |0\rangle + |1\rangle)/\sqrt{3}$. The ellipticity is $\varepsilon = 0$ (linear polarization) and the rotation angle is $\beta = 0$. The dotted curve shows the total population in sublevels $m_e = -1$ and 1 (the upper states in the V system, the total population in which is $\frac{1}{3}$), whereas the dashed curve shows the total population in sublevels $m_e = -2, 0, 2$ (the upper states in the W system, the total population in which is $\frac{2}{3}$). The solid curve shows the total population in all five excited sublevels.

cause nonlinear processes and ensuing loss of population. With pulses of a few-nanosecond duration, however, the required intensity for a π-pulse is of the order of 100 MHz for which nonlinear processes are generally negligible. We note that our frequent statements of "sufficiently" long sequences are supposed to comply with such restrictions, i.e. they cannot be infinitely long. However, one of the advantages of composite sequences if that relatively short sequences, of 3 to 10 pulses, usually suffice to dramatically change the excitation profile in a desired manner. We note that it is also possible to design composite sequences, in which each individual pulse has a smaller pulse area than π; to this end, we have added in Fig. 7 an example of a composite sequence of 5 pulses with area $3\pi/7$. Composite sequences of pulses of even smaller areas can be constructed, if needed.

Regarding the Majorana model, an implementation of a Majorana ladder of more than 3 states is beyond experimental reality in atoms, particularly regarding the strict conditions on the couplings. However, the Majorana model appears naturally in other situations, for example in rf transitions between magnetic sublevels in Bose-Einstein condensates and output couplers for atom lasers [27], and also in multiparticle systems in quantum information where subspaces of multiqubit states corresponding to a well-defined pseudospin can be separated, e.g. in trapped ions [37]. Of course, the Majorana model does not necessarily demand a ladder system; the three-state Λ-linkage realization is easily found in atoms, for example, the Zeeman-shifted magnetic sublevels $m_g = -1$ and $m_g = 1$ of a ground level with $J_g = 1$ coupled to the sublevel $m_e = 0$ of an upper level with $J_e = 1$ (or 0). There are numerous other examples of real physical systems, beyond the examples listed above, in which our results are applicable and potentially useful and important.

Another important experimental limitation is that the intensity of the pulses is limited by the splittings in the hyperfine energy levels. For the potassium and rubidium D-lines these splittings are large enough to allow the application of nanosecond pulses without affecting unwanted hyperfine levels [36]. The exemplary transition considered by us, $J_g = 1 \leftrightarrow J_e = 2$, can be found in several isotopes of these atoms and spectral lines. For example, for the D_1 line of ^{87}Rb the hyperfine splitting of the upper level $5^2P_{1/2}$ is 814.5 MHz [36], which allows the application of Rabi frequencies as large as 300 MHz for rectangular pulses and even larger for smooth pulses (for which the power broadening is much smaller than for rectangular pulses [38]). This makes it possible to reduce the pulse duration to as little as 1 ns without affecting the unwanted $F = 2$ hyperfine level of the excited manifold. For the D_2 line of ^{87}Rb the relevant splitting (between $F = 2$ and $F = 1$) is 157 MHz [36] and it imposes a lower limit of about 4-5 ns on the pulse duration. We note that with the composite sequences of $3\pi/7$ pulses mentioned above and shown in Fig. 7, the pulse duration can be reduced by a factor of 2 compared to the standard sequences of π pulses. Therefore, sequence of 3, 5, 7, and even 9 pulses can be made shorter that the lifetime of about 27 ns of the upper level of the D_1 and D_2 lines of ^{87}Rb. The limiting factor therefore is the time resolution achievable by the phase shifters, e.g. acoustooptic or electrooptic modulators [40].

We note that the technique is not limited to alkali atoms where the lifetimes of the upper levels in the D-lines are relatively short [36, 39]. We also note that the described application for population inversion in MS systems is by no means limited to $J_g = 1 \leftrightarrow J_e = 2$ transitions; it can be applied to any transition between J_g and $J_e = J_g + 1$, e. g. $F = 3 \leftrightarrow F = 2$ and $F = 4 \leftrightarrow F = 3$ transitions in the D1 and D2 lines of ^{133}Cs. There is no limitation to integer angular momentum values either: the angular momenta can also be half-integers.

VI. CONCLUSION

The powerful technique of composite pulse sequences is almost entirely designed for two-state quantum systems. We have described some applications of composite pulses to two types of multistate systems: systems with SU(2) dynamic symmetry and systems with MS symmetry. Both of these can be reduced to one or more effective two-state systems thereby making possible the use of the vast pool of composite pulses. We have given examples for some applications of BB, PB, and NB composite pulses for coherent manipulation of such systems. For SU(2)-symmetric systems, composite pulses allow one to stabilize the population inversion against variations in the pulse area and the detuning (with BB pulses), or to achieve enhanced selectivity of excitation (with NB pulses) or both (with PB pulses). For multistate systems with MS symmetry, composite pulses allow one to drive simultaneously several parallel linkage chains with nearly perfect efficiency. We have demonstrated how one can achieve perfect population inversion between two sets of degenerate states regardless of the initial population distribution in the lower set of states. Finally, we have discussed some important issues related to the experimental feasibility of the composite pulses technique.

Acknowledgments

This work is supported by the European Commission network FASTQUAST, and the Bulgarian NSF grants D002-90/08 and DMU02-19/09.

[1] M. H. Levitt and R. Freeman, J. Magn. Reson. **33**, 473 (1979).
[2] R. Freeman, S. P. Kempsell, and M. H. Levitt, J. Magn. Reson. **38**, 453 (1980).
[3] M. H. Levitt, J. Magn. Reson. **48**, 234 (1982).
[4] R. Tycko, Phys. Rev. Lett. **51**, 775 (1983); R. Tycko, A. Pines, and J. Guckenheimer, J. Chem. Phys. **83**, 2775 (1985).
[5] H. M. Cho, R. Tycko, A. Pines, and J. Guckenheimer, Phys. Rev. Lett. **56**, 1905 (1986).
[6] M. H. Levitt, Prog. NMR Spectrosc. **18**, 61 (1986).
[7] S. Wimperis, J. Magn. Reson. **109**, 221 (1994).
[8] R. Freeman, *Spin Choreography* (Spektrum, Oxford, 1997).
[9] B.T. Torosov and N.V. Vitanov, Phys. Rev. A 83, 053420(7) (2011)
[10] S. S. Ivanov and N. V. Vitanov, Opt. Lett. **36**, 7 (2011).
[11] H. Häffner, C.F. Roos, and R. Blatt, Phys. Rep. **469**, 155 (2008).
[12] I. Roos and K. Mølmer, Phys. Rev. A, **69**, 022321 (2004).
[13] C.D. Hill, Phys. Rev. Lett., **98**, 180501 (2007).
[14] S. S. Ivanov and N. V. Vitanov, Phys. Rev. A **84**, 022319 (2011).
[15] B.T. Torosov, S. Guérin and N.V. Vitanov, Phys. Rev. Lett. **106**, 233001 (2011).
[16] M. Born and E. Wolf, *Principles of Optics* (Pergamon, Oxford, 1975); M. A. Azzam and N. M. Bashara, *Ellipsometry and Polarized Light* (North Holland, Amsterdam, 1977); D. Goldstein and E. Collett, *Polarized Light* (CRC Press, 2003).
[17] C. D. West and A. S. Makas, J. Opt. Soc. Am. **39**, 791 (1949).
[18] M. G. Destriau and J. Prouteau, J. Phys. Radium **10**, 53 (1949).
[19] S. Pancharatnam, Proc. Ind. Acad. Sci. **51**, 130 (1955); ibid. **51**, 137 (1955).
[20] S. E. Harris, E. O. Ammann, and A. C. Chang, J. Opt. Soc. Am **54**, 1267 (1964).
[21] C. M. McIntyre and S. E. Harris, J. Opt. Soc. Am **58**, 1575 (1968).
[22] M. Steffen, J. M. Martinis, and I. L. Chuang, Phys. Rev. B **68**, 224518 (2003)
[23] E. Majorana, Nuovo Cimento **9**, 43 (1932).
[24] J.R. Morris and B.W. Shore, Phys. Rev. A **27**, 906 (1983).
[25] F. Bloch and I. I. Rabi, Rev. Mod. Phys. **17**, 237 (1945).
[26] F.T. Hioe, J. Opt. Soc. Am. B **4**, 1327 (1987).
[27] N.V. Vitanov and K.A. Suominen, Phys. Rev. A **56**, R4377 (1997).
[28] N. Rosen and C. Zener, Phys. Rev. **40**, 502 (1932).
[29] J. P. Davis and P. Pechukas, J. Chem. Phys. **64**, 3129 (1976).
[30] G. S. Vasilev and N. V. Vitanov, Phys. Rev. A **70**, 053407 (2004).
[31] A.A. Rangelov, N.V. Vitanov, and B.W. Shore, Phys. Rev. A **74**, 053402 (2006).
[32] G.S. Vasilev, S.S. Ivanov, and N.V. Vitanov, Phys. Rev. A **75**, 013417 (2007).
[33] E.S. Kyoseva and N.V. Vitanov, Phys. Rev. A **73**, 023420 (2006).
[34] E. S. Kyoseva, N. V. Vitanov, and B. W. Shore, J. Mod. Opt. **54**, S393 (2007).
[35] N. V. Vitanov, J. Phys. B **33**, 2333 (2000); N. V. Vitanov, Z. Kis, and B. W. Shore, Phys. Rev. A **68**, 063414 (2003).
[36] D. A. Steck, http://steck.us/alkalidata.
[37] I. E. Linington and N. V. Vitanov, Phys. Rev. A **77**, 010302 (2008).
[38] N. V. Vitanov, B. W. Shore, L. P. Yatsenko, K. Böhmer, T. Halfmann, T. Rickes, and K. Bergmann, Opt. Commun. **199**, 117 (2001); T. Halfmann, T. Rickes, N. V. Vitanov, and K. Bergmann, Opt. Commun. **220**, 353 (2003).
[39] E. Gomez, S. Aubin, L. A. Orozco, and G. D. Sprouse, J. Opt. Soc. Am. B **21**, 2058 (2004).
[40] N. J. Berg and J. N. Lee, *Acousto-Optic Signal Processing, Theory and Implementation* (New York: Marcel Dekker, Inc., 1983)